Research Square

Preprints are preliminary reports that have not undergone peer review.
They should not be considered conclusive, used to inform clinical practice,
or referenced by the media as validated information.

Prediction of Ubiquitin-Specific Peptidase 8 Mutation in Adrenocorticotropic Hormone-Producing Pituitary Neuroendocrine Tumor using Magnetic Resonance Imaging: Original Article

Yukitomo Ishi
Hokkaido University
Taisuke Harada
Hokkaido University
Hiroaki Motegi
moccihiro@gmail.com

Hokkaido University
Hiroyuki Kobayashi
Kashiwaba Neurosurgical
Ryosuke Sawaya
Hokkaido University
Michinari Okamoto
Hokkaido University
Hiraku Kameda
Hokkaido University
Shigeru Yamaguchi
Hokkaido University
Kohsuke Kudo
Hokkaido University
Miki Fujimura
Hokkaido University

Research Article

Keywords:

Posted Date: November 19th, 2026

DOI: https://doi.org/10.21203/rs.3.rs-8468862/v1

License: This work is licensed under a Creative Commons Attribution 4.0 International License.
Read Full License

Additional Declarations: No competing interests reported.

Abstract

Background This study aimed to investigate the correlation between magnetic resonance imaging (MRI) findings and Ubiquitin-Specific Peptidase 8 (USP8) status in adrenocorticotropic hormone (ACTH)-producing pituitary neuroendocrine tumor (PitNETs). This study included patients clinically diagnosed with Cushing's disease or subclinical Cushing's disease and pathologically diagnosed with ACTH-producing PitNET. USP8 status was analyzed with Sangar sequencing. Tumor diameter, Knosp grade, tumor border, and contrast enhancement compared to the pituitary gland on the equilibrium phase of gadolinium-enhanced T1 weighted image (Gd-T1WI) were retrospectively analyzed on preoperative MRI. The contrast-enhanced grade was classified on Gd-T1WI as 0–3 based on the border and enhancement pattern, indicating undetectable, vague and enhanced, partially indecisive and less enhanced, and well-circumscribed and less enhanced, respectively. Results USP8 mutation was harbored in 7 of 20 cases with ACTH-producing PitNETs. No statistical difference was found in the maximum tumor diameter and Knosp grade between USP8-mutant and -wild cases, but all USP8-mutant tumors were <15 mm, while 4 of 13 cases with USP8-wild cases were >15 mm. All USP8-mutant cases were classified as contrast-enhanced grades 2 or 3, while 2 cases were unclassified due to large tumors, and 7 of 11 cases were grade 0 or 1. Contrast-enhanced grades 2 or 3 and maximum tumor diameters of <15 mm were strongly correlated with USP8 mutation ($p = 0.0114$, Fisher's exact test).

Conclusion USP8 mutation in ACTH-producing PitNET would be predicted focusing on tumor border, enhancement pattern, and maximum tumor diameter on Gd-T1WI of MRI.

INTRODUCTION

Cushing's disease (CD) is caused by excessive adrenocorticotropic hormone (ACTH) secretion from pituitary neuroendocrine tumors (PitNETs). CD symptoms include various Cushingoid appearances, with typical features, such as moon face, central obesity, dorsocervical fat pad, purple striae, thin skin or proximal myopathy, and atypical features such as hypertension, menstrual abnormalities, acne, hirsutism, peripheral edema, impaired glucose tolerance, osteoporosis, pigmentation, or mental abnormalities[1]. Cases with autonomy in ACTH secretion due to PitNET while lacking typical features of CD are classified as subclinical Cushing's disease (SCD)[1, 2].

Previous genetic studies revealed 19%–36% of ACTH-producing PitNETs in *ubiquitin-specific peptidase 8* (*USP8*) mutations[3–7]. The hot spot region at codon 715–720 in *USP8* has been reported[3, 6]. PAs harboring *USP8* mutation present higher activities of ACTH secretion compared with that with wild-type *USP8*[3, 8]. *USP8* mutation in ACTH-producing PitNET has been associated with higher somatostatin receptor 5 (SSTR5) expression, which suggested a favorable response to pasireotide, which is a somatostatin analog, for *USP8*-mutant cases[9][10]. Thus, *USP8* mutation detection would have clinical value in terms of predicting treatment responses and prognoses. *USP8* mutations can be identified by DNA sequencing, while an alternative approach for *USP8* mutation detection in clinical procedures, such as magnetic resonance imaging (MRI), may help develop treatment strategies.

Tumor localization in patients with ACTH-producing PitNETs is challenging because of various patterns of MRI findings in size and signal intensity although MRI is commonly applied for diagnosing ACTH-producing PitNETs[11]. To date, factors that affect MRI findings in ACTH-producing PitNETs, including CDs and SCDs, have not been elucidated. Thus, this study aimed to investigate the correlation between MRI findings and *USP8* mutation in ACTH-producing PitNETs.

METHODS

Patient population

This retrospective study included patients with ACTH-producing PitNET initially treated at our institute from 2004 to 2021. Patients clinically diagnosed as CD or SCD based on endocrinologic examinations in the department of endocrinology and pathologically diagnosed as ACTH-producing PitNET was exclusively included. Clinical diagnosis of CD and SCD was provided based on the previously reported diagnostic criteria[12–14]. This study obtained approval from the institutional review board before its initiation (015–0154, 018–0363). The requirement for informed consent was waived because this study was retrospective.

Genetic analysis

DNA extraction from frozen tumor tissue or formalin-fixed paraffin-embedded (FFPE) block, polymerase chain reaction (PCR), and Sanger sequencing were performed as previously described[15]. Samples in which the presence of tumor tissue was pathologically confirmed were selected for DNA extraction from FFPE. The following PCR primers were used for screening of codon 715–720 of *USP8*: forward (5'-TATGTACCCACCGGAAATGG-3') and reverse (5'- TGGAGTTACTGTTGGCTTCC-3').

Assessment of MRI findings

Preoperative gadolinium-enhanced T1 weighted image (Gd-T1WI) with 1.5-T or 3-T MRI was retrospectively analyzed. Blinded MRI assessment for the genetic analysis was performed by a certificated neuroradiologist (13 years of experience). The maximum tumor diameter was measured using the dynamic and equilibrium phases of Gd-T1WI, and the tumor extent was assessed based on Knosp grade[16]. The contrast-enhanced grades of the equilibrium phase of Gd-T1WI were classified based on the tumor borders and the degree of tumor enhancement compared to the surrounding normal pituitary gland as 3 (well-circumscribed and less enhanced), 2 (partially vague but recognizable as a less-enhanced lesion), 1 (vague and enhanced but the presence of the tumor was obvious), and 0 (undetectable in the equilibrium phase) (Fig. 1). The maximum tumor was measured based on dynamic contrast-enhanced T1WI in cases with contrast-enhanced grades 1 or 0.

Statistical analysis

Statistical analysis was performed using Graphpad Prism 8 (GraphPad Software, San Diego, CA). A *p*-value of < 0.05 derived using the Fisher's exact test and Mann–Whitney U test was considered statistically significant.

RESULTS

Patient demographics and USP8 mutations

This study analyzed 20 patients, including 17 with CD and 3 with SCD (Table 1). *USP8* mutation was detected in 7 (35.0%) patients, including 6 (35.3%) with CD and 1 (33.3%) with SCD. Among 7 cases with *USP8* mutation, the following mutations were observed: p.S718P in 3 cases, p.S719del in 2 cases, and p.S718F and p.S718C in 1 case. All 7 cases with *USP8* mutation were female; however, 12 of 13 cases with wild-type *USP8* were female and with no statistical significance in gender between *USP8*-mutant and -wild cases ($p > 0.9999$, Fisher's exact test). The median age at the surgery was 36 and 49 years in *USP8*-mutant and wild cases, respectively, with no statistical significance ($p = 0.4496$, Mann–Whitney U test).

Table 1
Summary of cases with ACTH-producing PA analyzed in this study

Number of cases	**USP8-mutant**	**USP8-wild**	***P*-value**
	7	**13**	**–**
Age (years, median [range])	36 (17–63)	49 (15–71)	0.4496
Gender (male / female)	0/7	1/12	> 0.9999
Maximum tumor diameter (mm, median [range])	8.5 (6.7–13.8)	11.2 (4.8–52.3)	0.5748
Knosp grade 0–2 / 3–4	7/0	10/3	0.1680
[+] Contrast-enhanced-grade 0–1/2–3	0/7	7/4	*0.0128
[+] Two cases with large tumors were excluded due to the invisibility of the normal pituitary gland.			
[*] p < 0.05			
Statistical analysis: Mann–Whitney U test for age and maximum tumor diameter, and Fisher's exact test for gender, Knosp grade (grade 0–2 vs 3–4) and Contrast-enhanced grade (0–1 vs. 2–3).			

Size of ACTH-producing PitNET and USP8 status

The maximum tumor diameter (median [range]) was 8.5 (6.7–13.8) mm and 11.2 (4.8–52.3) mm in *USP8*-mutant and -wild cases, respectively, with no statistical difference (Table 1, Fig. 2A). All seven

cases with *USP8* mutation have < 15 mm, while 4 out of 13 cases with wild-type USP8 have > 15 mm of maximum tumor diameter. The difference in Knosp grade between *USP8*-mutant and -wild cases was not statistically significant, but 3 cases with *USP8*-wild cases presented with cavernous sinus extension with Knosp grades 3 and 4, while all the *USP8*-mutant cases presented tumors located within the pituitary fossa with Knosp grades 0–2 (Table 1, Supplementary Table, Fig. 2B).

Contrast-enhanced grade and USP8 status

The equilibrium phase of Gd-T1WI of MRI revealed that all 7 cases with *USP8* mutation presented well-circumscribed tumor border or obvious less-enhanced lesions and were relatively easy to detect as less-enhanced lesions compared with the pituitary gland (Fig. 3A. Supplementary Fig. 1). However, the majority of tumors with *USP8*-wild tended to be difficult to detect (Fig. 1, Fig. 3B, and Supplementary Fig. 2). All *USP8*-mutant cases were classified as grades 2 or 3, while 2 cases in *the USP8-wild* group were undetectable for the normal pituitary gland due to large tumors, and 7 out of 11 cases were classified as grade 0 or 1 on contrast-enhanced grade (Fig. 4, Table 1, Supplementary Table). Differences in the ratio of cases with contrast-enhanced grade 2/3 and 0/1 between *USP8*-mutant and -wild cases were statistically significant ($p = 0.0128$) (Table 1). A combination of maximum tumor diameter of < 15 mm, with maximum tumor diameter and contrast-enhanced grade, including two cases with large tumors in which contrast-enhanced grade could not be classified, contrast-enhanced grade 2 or 3 were strongly correlated with *USP8* mutation, considering the range of tumor size ($p = 0.0031$, Table 2).

Table 2
Correlation of *USP8* status and MRI findings in this study

N = 20		Maximum tumor diameter and contrast-enhanced grade	
		< 15 mm and grade 2/3	> 15 mm and/or grade 0/1
USP8	Mutant	7	0
	Wild-type	3	10
$p = 0.0031$ (Fisher's exact test)			

DISCUSSION

Previous reports revealed that the *USP8* mutation is associated with a smaller tumor diameter on MRI[3, 6], and cavernous sinus invasion was associated with wild-type *USP8* and *TP53* mutations[17]. Similar trends in tumor diameter and Knosp grade were observed in this study although it was not statistically significant, which would be due to the small number of cases included in this study. However, some cases with wild-type *USP8* presented a small tumor diameter the same as *USP8*-mutant cases, which suggests that the tumor diameter is not an independently strong predictive factor of *USP8* mutation.

Our study focused on the signal intensity compared to the surrounding normal pituitary grand on Gd-T1WI in addition to the maximum tumor diameter. *USP8*-mutant tumors presented well-circumscribed border or obvious less-enhanced lesions on the equilibrium phase of Gd-T1WI. We consider that *the USP8* mutation would be predictable with high accuracy from preoperative MRI in combination with the maximum tumor diameter and tumor border assessment using contrast-enhanced grade. This hypothesis has not been reported in pituitary tumors, but several reports have indicated the correlation of genotype and radiological findings in various central nervous tumors such as glioblastomas[18, 19], diffuse lower-grade gliomas[20–22], pediatric low-grade gliomas[23–25], craniopharyngiomas[26, 27], medulloblastomas[28], or metastatic tumors[29]. A recent study revealed the likelihood of surgical remission in *USP8*-mutant cases[5]. We speculate that the radiological findings in *USP8*-mutant cases may be associated with favorable preoperative detectability and result in favorable surgical remission, considering our results of radiological characteristics and corresponding *USP8* status.

Because this study included limited cases, further study with a large number of cases would be necessary to validate the efficacy of MRI findings to predict *USP8* mutation. In addition, a subset of *USP8*-wild cases presented small tumor diameter and well-circumscribed border as well as *USP8*-mutant cases in this study. Further exploration of MRI parameters that distinguish *USP8* status should be considered.

The mechanism of the correlation between MRI findings and *USP8* mutation remains unclear. *USP8* mutations cause cleavage of USP8 protein that results in elevated deubiquitinase activity and increased recycling of endocytosed epidermal growth factor receptor (EGFR)[6]. EGFR amplification in glioblastomas has been associated with a higher ratio of T2-bright volume to enclosed T1-enhancing volume and a fuzzy border on T2-WI[30]. *Ubiquitin-specific peptidase 48* (*USP48*) mutation has been frequently observed in *USP8*-wild cases[31]. EGFR upregulation caused by the *USP8* mutation activates mitogen-activated protein kinase signaling[3], while *the USP48* mutation results in NF-κB signaling activation[31]. We consider that such differences in altered signaling pathways caused by genetic alterations would result in differences in factors such as intratumoral vascular structure and result in the difference in enhancement patterns on MRI[32, 33].

Previous genetic analysis for *USP8* have been mainly performed for CDs[3, 6]; however, the incidence of *USP8* mutation in SCDs have been uncertain. A subset of SCDs, as well as our series, have presented *USP8* mutation[34, 35], which suggested the necessity of genetic analysis of *USP8*, including SCD cases. Additionally, our results suggest that *USP8*-mutant SCD cases present similar MRI findings with *USP8*-mutant CD cases.

Recently, various kinds of small molecules targeting genetic alterations have been applied for central nervous tumors[36]. The efficacy of targeting inhibition of *USP8* or associated EGFR pathway using USP8 inhibitor or HSP90 inhibitor, respectively, has been reported in *USP8*-mutant ACTH-producing PitNETs[37, 38]. Higher intratumoral T-cell infiltration caused by *USP8* mutation in ACTH-producing PitNETs, which was considered to predict immunotherapy responsiveness, has been reported in the view of tumor

immunotherapy[39]. Radiological *USP8* mutation prediction would provide useful information to predict the candidates for such targeting therapy in patients with ACTH-producing PitNETs.

CONCLUSIONS

ACTH-producing PitNET with *USP8* mutation presented a small tumor diameter and well-circumscribed border or obvious less-enhanced lesion on the equilibrium phase of Gd-T1WI. Preoperative diagnosis of *USP8* status would impact the surgical strategy for ACTH-producing PitNETs and might predict candidates for targeting therapy for *USP8* mutation in the future.

Declarations

Conflicts of interest

The authors declare no conflicts of interest.

Ethical approval

This study obtained approval from the institutional review board before its initiation (015–0154, 018–0363).

Author Contribution

Conceptualization: YI, TH, HMMethodology: YI, THResources: YI, TH, HM, HK, RS, MO, KH, YS, KKFormal analysis and investigation: YI, THOriginal draft preparation: YISupervision: MFAll authors reviewed and approved the final version of the manuscript.

Acknowledgement

The authors would like to thank Enago (www.enago.jp) for the English language review.

References

1. Kageyama K, Oki Y, Sakihara S, Nigawara T, Terui K, Suda T. Evaluation of the diagnostic criteria for Cushing's disease in Japan. Endocr J. 2013;60:127–35.
2. Tamada D, Kitamura T, Otsuki M, Oshino S, Saitoh Y, Shimomura I. Clinical significance of screening for subclinical Cushing's disease in patients with pituitary tumors. Endocr J. 2016;63:47–52.
3. Ma ZY, Song ZJ, Chen JH, et al. Recurrent gain-of-function USP8 mutations in Cushing's disease. Cell Res. 2015;25:306–17.

4. Lasolle H, Elsensohn MH, Wierinckx A, et al. Chromosomal instability in the prediction of pituitary neuroendocrine tumors prognosis. Acta Neuropathol Commun. 2020;8:190.
5. Losa M, Mortini P, Pagnano A, Detomas M, Cassarino MF, Pecori Giraldi F. Clinical characteristics and surgical outcome in USP8-mutated human adrenocorticotropic hormone-secreting pituitary adenomas. Endocrine. 2019;63:240–6.
6. Reincke M, Sbiera S, Hayakawa A, et al. Mutations in the deubiquitinase gene USP8 cause Cushing's disease. Nat Genet. 2015;47:31–8.
7. Perez-Rivas LG, Theodoropoulou M, Ferraù F, et al. The Gene of the Ubiquitin-Specific Protease 8 Is Frequently Mutated in Adenomas Causing Cushing's Disease. J Clin Endocrinol Metab. 2015;100:E997–1004.
8. Sesta A, Cassarino MF, Terreni M, et al. Ubiquitin-Specific Protease 8 Mutant Corticotrope Adenomas Present Unique Secretory and Molecular Features and Shed Light on the Role of Ubiquitylation on ACTH Processing. Neuroendocrinology. 2020;110:119–29.
9. Hayashi K, Inoshita N, Kawaguchi K, et al. The USP8 mutational status may predict drug susceptibility in corticotroph adenomas of Cushing's disease. Eur J Endocrinol. 2016;174:213–26.
10. Albani A, Perez-Rivas LG, Tang S, et al. Improved pasireotide response in USP8 mutant corticotroph tumours in vitro. Endocr Relat Cancer. 2022;29:503–11.
11. Chatain GP, Patronas N, Smirniotopoulos JG, et al. Potential utility of FLAIR in MRI-negative Cushing's disease. J Neurosurg. 2018;129:620–8.
12. Nieman LK, Biller BM, Findling JW, et al. The diagnosis of Cushing's syndrome: an Endocrine Society Clinical Practice Guideline. J Clin Endocrinol Metab. 2008;93:1526–40.
13. Oki Y, Hashimoto K, Hirata Y, et al. Development and validation of a 0.5 mg dexamethasone suppression test as an initial screening test for the diagnosis of ACTH-dependent Cushing's syndrome. Endocr J. 2009;56:897–904.
14. Suda T, Kageyama K, Nigawara T, Sakihara S. Evaluation of diagnostic tests for ACTH-dependent Cushing's syndrome. Endocr J. 2009;56:469–76.
15. Ishi Y, Takamiya S, Seki T et al. Prognostic role of H3K27M mutation, histone H3K27 methylation status, and EZH2 expression in diffuse spinal cord gliomas. Brain Tumor Pathol. 2020.
16. Knosp E, Steiner E, Kitz K, Matula C. Pituitary adenomas with invasion of the cavernous sinus space: a magnetic resonance imaging classification compared with surgical findings. Neurosurgery. 1993;33:610-7; discussion 7–8.
17. Perez-Rivas LG, Simon J, Albani A, et al. TP53 mutations in functional corticotroph tumors are linked to invasion and worse clinical outcome. Acta Neuropathol Commun. 2022;10:139.
18. Li Y, Liang Y, Sun Z, et al. Radiogenomic analysis of PTEN mutation in glioblastoma using preoperative multi-parametric magnetic resonance imaging. Neuroradiology. 2019;61:1229–37.
19. Natsumeda M, Chang M, Gabdulkhaev R et al. Predicting BRAF V600E mutation in glioblastoma: utility of radiographic features. Brain Tumor Pathol. 2021.

20. Arita H, Kinoshita M, Kawaguchi A, et al. Lesion location implemented magnetic resonance imaging radiomics for predicting IDH and TERT promoter mutations in grade II/III gliomas. Sci Rep. 2018;8:11773.
21. Park YW, Han K, Ahn SS, et al. Prediction of IDH1-Mutation and 1p/19q-Codeletion Status Using Preoperative MR Imaging Phenotypes in Lower Grade Gliomas. AJNR Am J Neuroradiol. 2018;39:37–42.
22. Park YW, Ahn SS, Park CJ, et al. Diffusion and perfusion MRI may predict EGFR amplification and the TERT promoter mutation status of IDH-wildtype lower-grade gliomas. Eur Radiol. 2020;30:6475–84.
23. Trasolini A, Erker C, Cheng S et al. MR Imaging of Pediatric Low-Grade Gliomas: Pretherapeutic Differentiation of BRAF V600E Mutation, BRAF Fusion, and Wild-Type Tumors in Patients without Neurofibromatosis-1. AJNR Am J Neuroradiol. 2022.
24. Shrot S, Kerpel A, Belenky J, Lurye M, Hoffmann C, Yalon M. MR Imaging Characteristics and ADC Histogram Metrics for Differentiating Molecular Subgroups of Pediatric Low-Grade Gliomas. AJNR Am J Neuroradiol. 2022.
25. Ishi Y, Yamaguchi S, Yoshida M et al. Correlation between magnetic resonance imaging characteristics and BRAF alteration status in individuals with optic pathway/hypothalamic pilocytic astrocytomas. J Neuroradiol. 2019.
26. Yue Q, Yu Y, Shi Z, et al. Prediction of BRAF mutation status of craniopharyngioma using magnetic resonance imaging features. J Neurosurg. 2018;129:27–34.
27. Zhu W, Tang T, Yuan S, Chang B, Li S, Chen M. Prediction of CTNNB1 Mutation Status in Pediatric Cystic Adamantinomatous Craniopharyngioma by Using Preoperative Magnetic Resonance Imaging Manifestation. Clin Neurol Neurosurg. 2021;200:106347.
28. Reis J, Stahl R, Zimmermann H, et al. Advanced MRI Findings in Medulloblastomas: Relationship to Genetic Subtypes, Histopathology, and Immunohistochemistry. J Neuroimaging. 2021;31:306–16.
29. Wang G, Wang B, Wang Z, et al. Radiomics signature of brain metastasis: prediction of EGFR mutation status. Eur Radiol. 2021;31:4538–47.
30. Aghi M, Gaviani P, Henson JW, Batchelor TT, Louis DN, Barker FG 2. Magnetic resonance imaging characteristics predict epidermal growth factor receptor amplification status in glioblastoma. Clin cancer research: official J Am Association Cancer Res. 2005;11:8600–5.
31. Chen J, Jian X, Deng S, et al. Identification of recurrent USP48 and BRAF mutations in Cushing's disease. Nat Commun. 2018;9:3171.
32. Hervey-Jumper SL, Garton HJ, Lau D, et al. Differences in vascular endothelial growth factor receptor expression and correlation with the degree of enhancement in medulloblastoma. J Neurosurg Pediatr. 2014;14:121–8.
33. Leenders W, Küsters B, Pikkemaat J, et al. Vascular endothelial growth factor-A determines detectability of experimental melanoma brain metastasis in GD-DTPA-enhanced MRI. Int J Cancer. 2003;105:437–43.

34. Bujko M, Kober P, Boresowicz J, et al. USP8 mutations in corticotroph adenomas determine a distinct gene expression profile irrespective of functional tumour status. Eur J Endocrinol. 2019;181:615–27.
35. Uzilov AV, Taik P, Cheesman KC, et al. USP8 and TP53 Drivers are Associated with CNV in a Corticotroph Adenoma Cohort Enriched for Aggressive Tumors. J Clin Endocrinol Metab. 2021;106:826–42.
36. Mukasa A. Genome Medicine for Brain Tumors: Current Status and Future Perspectives. Neurol Med Chir (Tokyo). 2020;60:531–42.
37. Kageyama K, Asari Y, Sugimoto Y, Niioka K, Daimon M. Ubiquitin-specific protease 8 inhibitor suppresses adrenocorticotropic hormone production and corticotroph tumor cell proliferation. Endocr J. 2020;67:177–84.
38. Shen Y, Ji C, Jian X, et al. Regulation of the EGFR Pathway by HSP90 Is Involved in the Pathogenesis of Cushing's Disease. Front Endocrinol (Lausanne). 2020;11:601984.
39. Wang Z, Guo X, Gao L, et al. The Immune Profile of Pituitary Adenomas and a Novel Immune Classification for Predicting Immunotherapy Responsiveness. J Clin Endocrinol Metab. 2020;105:e3207–23.

Figures

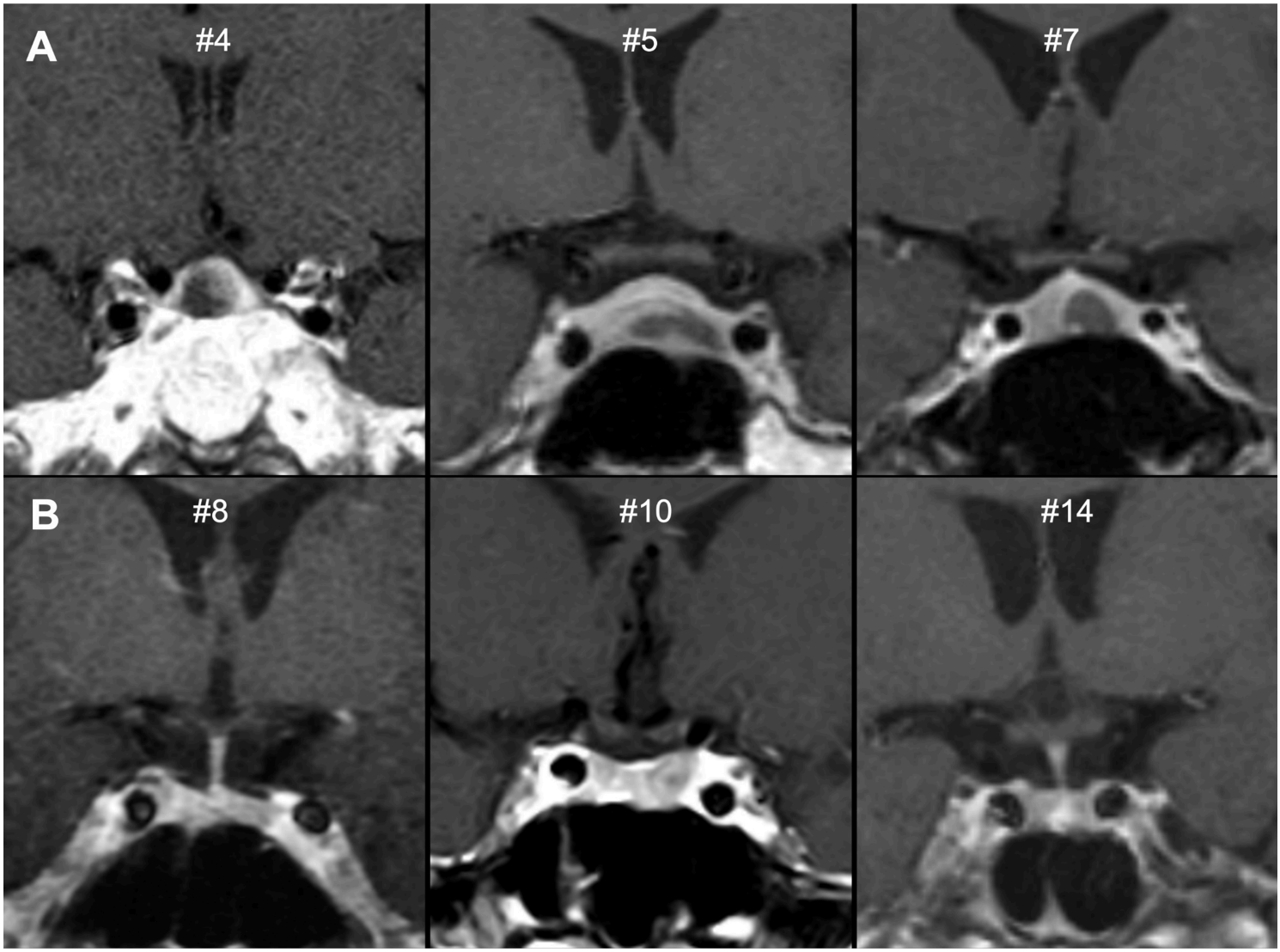


Figure 3

Representative images of Gd-T1WI (coronal view) in *USP8*-mutant and -wild cases.

(A) Gd-T1WI of *USP8*-mutant cases. (Left) Case #4, with CD, right-sided tumor, and contrast-enhanced grade 3. (Middle) Case #5, with CD, left-sided tumor, and contrast-enhanced grade 3. (Right) Case #7, with SCD, left-sided tumor, and contrast-enhanced grade 3.

(B) Gd-T1WI of *USP8*-wild cases. (Left)Case #8, with CD, left-sided tumor, and contrast-enhanced grade 0. (Middle) Case #10, with CD, left-sided tumor, and contrast-enhanced grade 0. (Right) Case #114, with CD, right-sided tumor, and contrast-enhanced grade 0.

Supplementary Files

This is a list of supplementary files associated with this preprint. Click to download.

- SupplementaryMaterial.pdf

- SupplementaryTable.pdf
- SupplementaryFigure2.jpeg
- SupplementaryFigure1.jpeg